Excitability of the Soma in Central Nervous System Neurons

Boris V. Safronov, Matthias Wolff, and Werner Vogel
Physiologisches Institut, Justus-Liebig-Universität Giessen, Aulweg 129, 35392 Giessen, Germany

ABSTRACT The ability of the soma of a spinal dorsal horn neuron, a spinal ventral horn neuron (presumably a motoneuron), and a hippocampal pyramidal neuron to generate action potentials was studied using patch-clamp recordings from rat spinal cord slices, the "entire soma isolation" method, and computer simulations. By comparing original recordings from an isolated soma of a dorsal horn neuron with simulated responses, it was shown that computer models can be adequate for the study of somatic excitability. The modeled somata of both spinal neurons were unable to generate action potentials, showing only passive and local responses to current injections. A four- to eightfold increase in the original density of Na^+ channels was necessary to make the modeled somata of both spinal neurons excitable. In contrast to spinal neurons, the modeled soma of the hippocampal pyramidal neuron generated spikes with an overshoot of +9 mV. It is concluded that the somata of spinal neurons cannot generate action potentials and seem to resist their propagation from the axon to dendrites. In contrast, the soma of the hippocampal pyramidal neuron is able to generate spikes. It cannot initiate action potentials in the intact neurons, but it can support their back-propagation from the axon initial segment to dendrites.

INTRODUCTION

The soma of central neurons plays an important role in determining their firing behavior. The studies of mechanisms of the action potential generation have mainly focused on functions of the axon initial segment (Coombs et al., 1957a,b; Eccles, 1964) and recently on the properties of dendrites (Stuart and Sakmann, 1994; Johnston et al., 1996). It has been shown that the action potentials are initiated in the axon (Coombs et al., 1957a,b; Eccles, 1964; Stuart and Sakmann, 1994; Safronov et al., 1997; Safronov, 1999) and spread passively (Stuart and Hausser, 1994) or actively (Stuart and Sakmann, 1994) into the dendritic tree. Contributions of the soma of central nervous system (CNS) neurons to spike initiation and propagation, however, is not sufficiently understood. The major difficulty in studying the excitability of the soma has been its close attachment to the axon initial segment, so that the relative contributions of the soma and the axon to the action potential could not be clearly distinguished. Using the "entire soma isolation" (ESI) method (Safronov et al., 1997), we succeeded in separating the soma (diameter of 8–12 μm) of a spinal dorsal horn neuron from the axon and the dendritic tree. It was found that the soma itself is not able to generate action potentials and plays a complex role in the excitability of the dorsal horn neuron (Wolff et al., 1998). The postnatal development of dorsal horn neurons was accompanied by additional expression of Na^+ channels in the axon initial segment rather than in the cell soma, so that the somata of older animals remained inexcitable (Safronov et al., 1999). The purpose of the present study was to show how far these conclusions are applicable to different types of CNS neurons. For comparison, we chose the spinal motoneuron and the hippocampal pyramidal neuron whose large somata, with a diameter of 20–30 μm, could not be directly isolated by means of the ESI method.

By comparing the original recordings from an ESI-isolated soma of a dorsal horn neuron with computer-simulated responses, we show that the modeling can be adequately used for investigation of the excitability of the soma. Further simulations of somatic responses have shown that the somata of spinal neurons are not able to generate action potentials. The experimentally measured density of Na^+ channels was at least four to eight times lower than that needed for the soma membrane to become excitable. In contrast, the modeled soma of a pyramidal neuron could generate action potentials. The influence of the soma on conduction in spinal and pyramidal neurons is discussed.

MATERIALS AND METHODS

Preparation

Experiments were performed by means of the patch-clamp technique (Hamill et al., 1981) on 150- or 200-μm slices (Edwards et al., 1989) prepared from the lumbar enlargement (L3–6) of the spinal cord of 4–15-day-old rats. Rats were rapidly decapitated, and the spinal cords were carefully cut out. This procedure was approved by the local veterinary authority (Regierungspräsidium Giessen). The slices were prepared and kept according to a description given by Takahashi (1990). The ESI experiments were carried out on dorsal horn neurons with a soma diameter of 8–12 μm (laminae I–III) identified and separated from glial cells by a procedure described previously (Safronov et al., 1997). The patch-clamp recordings were performed on the soma of large ventral horn neurons with a mean diameter of the short and long axes exceeding 22 μm. According to retrograde staining experiments performed on newborn rats by Takahashi (1990), ventral horn neurons with mean soma diameters above 22 μm are most likely to be motoneurons. All experiments with motoneurons were carried out on 6-day-old rats, because the spinal cord slices from older animals contained only a very few large ventral horn neurons suitable for the patch-clamp investigation.

Received for publication 16 September 1999 and in final form 18 February 2000.

Address reprint requests to Dr. B.V. Safronov, Physiologisches Institut, Justus-Liebig-Universität Giessen, Aulweg 129, D-35392 Giessen, Germany. Tel.: +49-(0)641-99-47268; Fax: +49-(0)641-99-47269; E-mail: boris.safronov@physiologie.med.uni-giessen.de or safronov@ibmc.up.pt.

0006-3495/00/06/2998/13 $2.00

Solutions

Preparation solution also used to maintain the slices contained (in mM) 115 NaCl, 5.6 KCl, 2 $CaCl_2$, 1 $MgCl_2$, 11 glucose, 1 NaH_2PO_4, 25 $NaHCO_3$ (pH 7.4 when bubbled with a 95%/5% mixture of O_2/CO_2). To reduce synaptic activity in neurons, the slices in the experimental chamber were perfused with low-Ca^{2+}/high-Mg^{2+} solution, which was obtained from the preparation solution by setting the concentrations of Ca^{2+} and Mg^{2+} to 0.1 and 5 mM, respectively. The densities of Na^+ and K^+ channels in motoneurons were determined by recording from cell-attached patches. The external solution used for pipette filling in experiments with Na^+ channels (tetraethylammonium (TEA) solution) contained (in mM) 115.8 NaCl, 5.6 KCl, 0.1 $CaCl_2$, 5 $MgCl_2$, 11 glucose, 36 TEA-Cl, and 10 HEPES (pH 7.4 adjusted with NaOH to give a final concentration of 5.2 mM). The external 155 mM K^+ solution (high K_o) used for pipette filling in experiments with K^+ channels contained (in mM) 5 NaCl, 152.5 KCl, 2.2 $CaCl_2$, 1 $MgCl_2$, and 5 HEPES (the pH was adjusted to 7.4 with KOH, giving a final concentration of 2.5 mM). Tetrodotoxin (100 nM) was added to this solution to block voltage-gated Na^+ channels.

The internal solution (high K_i) contained (in mM) 5 NaCl, 144.4 KCl, 1 $MgCl_2$, 3 EGTA, and 10 HEPES (pH was adjusted to 7.3 with NaOH, giving a final concentration of 10 mM). All experiments were carried out at a room temperature of 21–24°C.

Current recordings

Patch pipettes were pulled from borosilicate glass tubes (GC 150; Clark Electromedical Instruments, Pangbourne, UK). The pipettes used for single-channel recordings from motoneurons were coated with Sylgard 184 (Dow Corning) and had a resistance of 1.5–3.5 MΩ. Pipettes for whole-cell recordings from dorsal horn neurons had a resistance of 2–7 MΩ. All pipettes were fire-polished directly before the experiments. The patch-clamp amplifier was a List EPC-7 (List, Darmstadt, Germany) in all voltage-clamp and current-clamp experiments. The effective corner frequency of the low-pass filter was 3 kHz in experiments with Na^+ channels and 1 kHz in the study of K^+ channels. The frequency of digitization was at least twice that of the filter in voltage-clamp recordings and 10 kHz in current-clamp experiments. The data were stored and analyzed with commercially available software (pCLAMP version 5.5.1; Axon Instruments, Foster City, CA). Transients and leakage currents were digitally subtracted using records with negative pulses. Offset potentials were nulled immediately before the formation of a seal.

The method of "entire soma isolation"

Responses of the soma of dorsal horn neurons were studied by means of the ESI method (Safronov et al., 1997). Briefly, in whole-cell recording mode, the entire soma of the neuron was isolated from the slice by slow withdrawal of the recording pipette. The isolated structure was classified as a *soma* if it had lost all of its processes during isolation. The isolated structure was classified as a *soma+axon* complex if it contained one process and preserved more than 90% of the original Na^+ current recorded in the slice before isolation. The good physiological state of the isolated structures was confirmed by a decrease in membrane leakage conductance, by stable or even improved membrane resting potentials, and by the ability of *soma+axon* complexes to generate action potentials (Safronov et al., 1997).

The present study is based on recordings from 20 isolated *somata* and from 22 cell-attached patches. All numerical values are given as mean ± SEM. The data points were fitted by linear or nonlinear least-squares procedures. The errors of the fitting parameters are given ± SE.

Computer simulation

Responses of the soma were simulated using the program Neuron, version 3.2.3 (Hines, 1993; Hines and Carnevale, 1997), with an integration step of 10–100 μs. The soma was considered as a cylinder with diameter and length of 10 and 10 μm for the dorsal horn neuron, 25 and 25 μm for the motoneuron, and 20 and 30 μm for the hippocampal pyramidal neuron, respectively. The simulations in Figs. 1, 2, 4, and 5 were carried out using experimental data obtained at a room temperature of 21–24°C, and those in Figs. 6–8 were carried out for 37°C (the temperature in simulations was increased by 14°C).

Passive membrane properties of somata

Responses of the soma were simulated using an axial resistance (R_i) of 200 Ωcm (Mainen et al., 1995). The membrane capacitance (C_M) was 1 μF/cm^2 in all simulations, except those of Fig. 2, where the best fitting of the original passive responses was achieved with $C_M = 2$ μF/cm^2. The influence of the R_i and C_M values on the results of our simulations is described in the Results section.

It was shown in the ESI experiments on dorsal horn neurons (Safronov et al., 1997) that the leakage current in the ESI-isolated soma (*soma*) was on the average ~50% of that recorded in the intact neuron before isolation. Because the resting potential in the *soma* was not lower than that in the intact neuron before isolation, it could be supposed that the isolation procedure did not result in a remarkable increase in nonspecific membrane conductance or seal conductance. In the present study, we therefore assumed that the soma has a leakage current that is approximately twice as small (or an input resistance, R_{IN}, that is twice as high) as that recorded from the intact neuron with the patch-clamp electrode placed on its soma. The passive membrane conductance was adjusted in the model to give a R_{IN} of 7 GΩ for the soma of the dorsal horn neuron (3.7 GΩ for the whole neuron; Safronov et al., 1997), 0.6 GΩ for the soma of the motoneuron (0.29 GΩ for the motoneuron; Takahashi, 1990), and 0.6 GΩ for the soma of the pyramidal neuron (0.2–0.4 GΩ for the CA3 neuron; Jonas et al., 1993). The corresponding values of the specific membrane resistivity (R_m) were 22,222 Ω cm^2 for a dorsal horn neuron, 12,121 Ω cm^2 for a motoneuron, and 11,236 Ω cm^2 for a pyramidal neuron. Because the ESI experiments provide no possibility of measuring exactly the reduction in the passive membrane conductance and seal conductance during the *soma* isolation (and, therefore, the possibility cannot be completely excluded that the value of R_{IN} assumed for the modeled soma considerably underestimates the real value), we designed control simulations in which the R_{IN} (or R_m) values were increased 10-fold. A 10-fold increase in the R_{IN} value did not result in the appearance of somatic excitability (see Results). The resting potential in modeled somata was determined by setting the equilibrium potential for the leakage conductance to −70 mV.

Na^+ currents

The Na^+ current (I_{Na}) was described by a standard equation (Hodgkin and Huxley, 1952), $I_{Na} = g_{Na}m^3h(E - E_{Na})$, where g_{Na} is the Na^+ conductance, m and h are the variables of activation and inactivation, respectively, E is the membrane potential, and $E_{Na} = +53$ mV is the equilibrium potential for Na^+. The simulation parameters were based on those used to model Na^+ currents in neocortical pyramidal neurons (Mainen et al., 1995). The steady-state activation variable (m_∞) and the time constant of activation (τ_m) were determined as $m_\infty = \alpha_m/(\alpha_m + \beta_m)$ and $\tau_m = 1/(\alpha_m + \beta_m)$, where α_m and β_m were forward and backward reaction rates, given as

$$\alpha_m = 0.182(E + 35)/(1 - \exp(-(E + 35)/9)),$$

$$\beta_m = -0.124(E + 35)/(1 - \exp((E + 35)/9)).$$

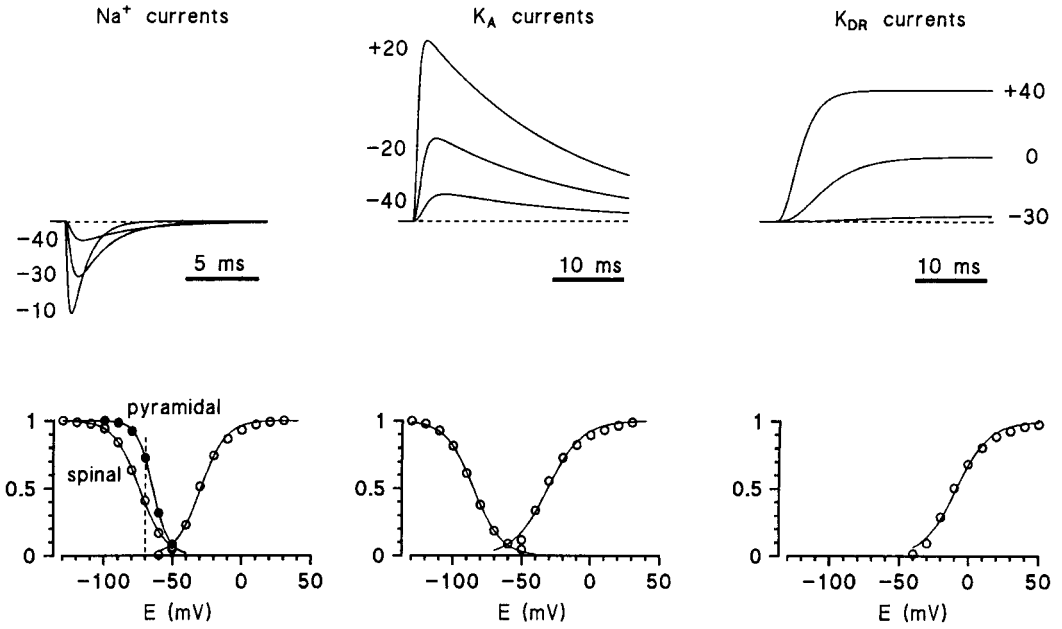

FIGURE 1 Simulated Na^+ and K^+ currents: kinetics and steady-state activation and inactivation characteristics of simulated Na^+, K_A, and K_{DR} currents. The steady-state inactivation characteristics of Na^+ channels in pyramidal (●) and spinal (○) neurons were modeled using different parameters (see Materials and Methods and Results). All other parameters of Na^+, K_A, and K_{DR} current models were assumed to be equal for the dorsal horn neuron, the motoneuron, and the pyramidal neuron. The fitting parameters of the steady-state activation and inactivation curves of simulated currents are given in the Results.

The time constant of inactivation (τ_h) was determined as $\tau_h = 1/(\alpha_h + \beta_h)$, where α_h and β_h are the forward and backward reaction rates:

$$\alpha_h = 0.024(E + 50)/(1 - \exp(-(E + 50)/5)),$$

$$\beta_h = -0.0091(E + 75)/(1 - \exp((E + 75)/5)).$$

The steady-state inactivation variable (h_∞) was determined by an equation,

$$h_\infty = 1/(1 + \exp((E - E_{H50})/k)),$$

where E_{H50} is the potential of half-maximum channel inactivation and k is a steepness factor. The E_{H50} was −65 mV and k was 6.2 mV for pyramidal neurons (Huguenard et al., 1988; Mainen et al., 1995). The inactivation parameters for both spinal neurons are determined in Results section.

Densities of Na^+ channels

The density of somatic Na^+ channels in dorsal horn neurons was estimated using our recordings from isolated *somata* (Safronov et al., 1997). The maximum Na^+ current activated in the *soma* after a hyperpolarizing prepulse to −120 mV was 272 ± 26 pA (46 *somata*). This value was obtained from that reported (306 ± 27 pA) for 52 *somata* after the exclusion of those six *somata* that preserved part of the steady-state Na^+ current and a relatively large inactivating Na^+ current and therefore probably contained part of the axon hillock. The maximum *soma* current of 272 pA corresponded to a Na^+ current density of 0.87 pA/μm^2 (soma area of 314 μm^2) activated by a voltage step from −120 to −10 mV in model neurons (potential at which the maximum inward Na^+ current was simulated).

In a pyramidal neuron, the current density was 3 pA/μm^2 at a voltage step from −90 to −10 mV (Colbert and Johnston, 1996). The current density in spinal motoneurons was set in accordance with the data presented in the Results.

K_A currents

Potassium K_A currents were uniformly modeled for all neurons. The model based on our recordings from the *soma* of a dorsal horn neuron (Wolff et al., 1998) was slightly modified to obtain the steady-state activation characteristics similar to those reported for K_A currents in a motoneuron (Safronov and Vogel, 1995) and a CA1 pyramidal neuron (Klee et al., 1995). K_A current ($I_{K(A)}$) was described as $I_{K(A)} = g_{K(A)}m^4h(E - E_K)$, where $g_{K(A)}$ is K_A conductance, m and h are activation and inactivation state variables, and E_K is −84 mV. The parameters were defined as follows: $m_\infty = \alpha_m/(\alpha_m + \beta_m)$, $h_\infty = \alpha_h/(\alpha_h + \beta_h)$, $\tau_m = 1/(\alpha_m + \beta_m)$, and $\tau_h = 1/(\alpha_h + \beta_h)$, where α_m, β_m, α_h, and β_h are

$$\alpha_m = 0.032(E + 64)/(1 - \exp(-(E + 64)/6)),$$

$$\beta_m = 0.203 \exp(-(E + 40)/24),$$

$$\alpha_h = 0.05/(1 + \exp((E + 86)/10)),$$

and

$$\beta_h = 0.05/(1 + \exp(-(E + 86)/10)).$$

According to these equations τ_h was 20 ms at all potentials.

Densities of K_A channels

The densities of K_A currents in dorsal horn neurons were determined using our recordings from isolated *somata*. The amplitude of the *soma* K_A current

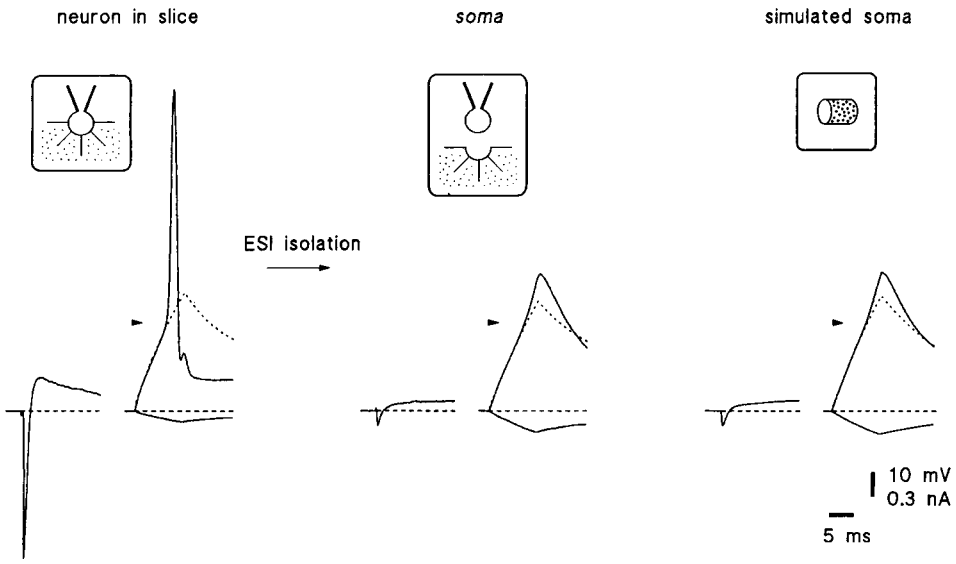

FIGURE 2 Membrane responses of an intact dorsal horn neuron, its isolated *soma*, and a simulated soma. Voltage-clamp and current-clamp recordings from an intact dorsal horn neuron in the spinal cord slice, from its isolated *soma* and from a simulated soma (15-day-old rat). In the voltage-clamp mode the membrane currents were activated by a step to −10 mV after a 50-ms prepulse to −120 mV. The holding potential was −80 mV. Under current-clamp conditions, the cells were held at −80 mV by injection of a steady-state current through the recording pipette. Hyperpolarizing (−10 pA) and then depolarizing current pulses were injected into the intact neuron (+110 pA), the isolated *soma* (+50 pA), and the simulated soma (+50 pA). The passive responses (indicated by *dashed lines*) were calculated for the intact neuron and the isolated *soma* by multiplying the membrane responses to negative (−10 pA) current pulses by appropriate factors, −11 and −5, respectively (Safronov et al., 1997), and for the simulated soma by setting all active conductances to zero. The simulation parameters were adjusted to achieve similarity between responses of the isolated *soma* and the simulated soma in both voltage-clamp and current-clamp experiments. The threshold of the action potential in the intact neuron is indicated by arrows in all traces. Recordings were made in low-Ca^{2+}-high-Mg^{2+} solution, using pipettes filled with high-K_i solution.

activated by a voltage step from −120 to +40 mV was 330 pA (Wolff et al., 1998), giving a current density of 1.05 pA/μm^2. For pyramidal neurons, the density of the K_A current was reported to be 8.32 pA per patch (10–20-MΩ pipettes) at a voltage step from −85 mV ($h_\infty \approx 1$) to +55 mV ($m_\infty^4 \approx 1$) (Hoffman et al., 1997). For a mean 15-MΩ pipette (1.1 μm^2 area; Sakmann and Neher, 1995) the corresponding current density will be 7.56 pA/μm^2. This density was used in our simulation at a voltage step from −120 mV ($h_\infty \approx 1$) to +55 mV ($m_\infty^4 \approx 1$). The K_A current density in a motoneuron is determined in the Results.

K_{DR} currents

The model for K_{DR} current was based on our recordings from an isolated *soma* of a dorsal horn neuron (Wolff et al., 1998) and was also used for the motoneuron and the pyramidal neuron. The parameters were adjusted slightly to resemble K_{DR} currents in CA1 pyramidal neurons (Klee et al., 1995). K_{DR} current ($I_{K(DR)}$) was described by the equation $I_{K(DR)} = g_{K(DR)} m^4 (E - E_K)$, where $g_{K(DR)}$ is the K_{DR} conductance. The steady-state activation variable and the time constant were defined as $m_\infty = \alpha_m/(\alpha_m + \beta_m)$ and $\tau_m = 1/(\alpha_m + \beta_m)$, where α_m and β_m are

$$\alpha_m = 0.0075(E + 30)/(1 - \exp(-(E + 30)/10))$$

and

$$\beta_m = 0.1 \exp(-(E + 46)/31).$$

Densities of K_{DR} channels

The *soma* K_{DR} current activated by a voltage pulse from −60 to +40 mV in a dorsal horn neuron was 240 pA (Wolff et al., 1998), giving a current density of 0.76 pA/μm^2. For a pyramidal neuron, the density of somatic currents of 8.39 pA per patch after a voltage step to +55 mV (Hoffman et al., 1997), reevaluated using a procedure similar to that used for K_A channels was 7.63 pA/μm^2. The density of the K_{DR} current in a motoneuron is determined in the Results.

Simulation of action potentials in a motoneuron of adult cat

To reproduce several observations made by Eccles and co-workers, action potential simulations were performed in adult cat motoneurons. The model of an adult cat motoneuron consisted of the soma, the axon hillock (AH), the axon initial segment (IS), and an equivalent dendrite (Fig. 6 *A*). The parameters of the model were set in agreement with the results of numerous anatomical measurements. The soma of an adult cat motoneuron was modeled as a 60-μm-long cylinder with a diameter of 60 μm (Ulfhake and Kellerth, 1983). The 15-μm-long AH linearly tapered in diameter from 13 μm at the base (Kellerth et al., 1979) to the diameter of the IS at its distal end. The IS had a constant diameter of 3.5 μm and a length of 30 μm (Cullheim and Kellerth, 1978). The dendritic tree of a motoneuron was represented by an equivalent dendrite of variable diameter (Rall, 1959; Clements and Redman, 1989; Fleshman et al., 1988; Jones and Bawa, 1997). According to anatomical measurements of different types of adult cat α-motoneurons (figure 9 from Fleshman et al., 1988), the diameters of the stem of an equivalent dendrite were in the range of 25.6–45.1 μm. An equivalent dendrite used in our simulations had a constant diameter of 35 μm for the first 3000 μm and linearly narrowed to zero over the next 4000 μm (total length 7000 μm). The electrotonic length of the dendrite was 2.5 λ. The soma, AH, IS, and an equivalent dendrite consisted of 10, 30, 50, and 50 compartments, respectively.

The R_i values reported for motoneurons are in the range of 70–87 Ω cm (Barrett and Crill, 1974; Thurbon et al., 1998). Our simulations were performed with $R_i = 80$ Ω cm. The C_M was assumed to be 1 μF/cm^2 for all compartments. To account for a somatic shunt resistance introduced by the recording electrode, the specific membrane resistivity (R_m) was nonuniform and was set in accordance with the step model of membrane resistivity (Clements and Redman, 1989; Fleshman et al., 1988). The R_m value was 222.2 Ω cm^2 for the soma, AH, and IS, and 7143 Ω cm^2 for the membrane of an equivalent dendrite. These R_m values were adjusted to give an input resistance of 1 MΩ when measured with long current pulses applied to the soma of a motoneuron. The membrane time constant (τ_0), determined in a modeled motoneuron by an exponential fitting of the slowest component of a voltage transient response to the injection of a sustained current into the soma (Rall, 1969), was ~5 ms, in the range typical for adult cat motoneurons studied using a sharp electrode (Burke and ten Bruggencate, 1971). The resting potential in a simulated motoneuron of an adult cat was determined by setting the equilibrium potential for the leakage conductance to −80 mV.

The action potentials in the isolated somata simulated with our models derived for Na^+ and K^+ currents recorded at a room temperature of 21–24°C had a duration of ~2–3 ms (see Figs. 4 and 5). Original action potentials recorded at 37°C in the axon initial segment of the adult cat motoneuron by Coombs et al. (1957a) lasted for ~1 ms. To shorten the simulated spikes to 1 ms, the temperature of simulation was increased to 37°C, in accordance with the temperature at which the measurements from Coombs et al. (1957a) were made. In this case, all rate constants of channel gating were uniformly multiplied by a coefficient $Q_{10}^{(37-23)/10}$. Assuming Q_{10} for gating reactions to be 3 (Frankenhaeuser and Moore, 1963), this coefficient was 4.66.

For reasons explained in the Results, the active conductances (Na^+ and K_{DR}) were inserted into the membranes of AH and/or IS only. The density of Na^+ current activated by a voltage pulse from −80 to −10 mV in both AH and IS was ~830 pA/μm^2 (~13,200 pS/μm^2), corresponding to the activation of ~530 channels/μm^2 with a conductance of 25 pS (37°C), obtained from the value of 14 pS (21–24°C) from Safronov and Vogel (1995), assuming a Q_{10} value for the single-channel conductance of 1.5 (Hille, 1992). This density was several times lower than those typically used in simulation studies for the axon initial segment (Mainen et al., 1995). It provided a maximum velocity of depolarization (320 V/s for the somatic membrane) similar to that measured by Coombs et al. (1957a). The amplitude of the whole-cell peak Na^+ current elicited in a motoneuron by a voltage step from −80 to −10 mV under conditions of sufficient voltage clamp (achieved by setting R_I to 0) was 0.61 μA. Of this total of 0.61 μA (IS + AH membrane area 738 μm^2), 0.27 μA was supplied by the IS (area 330 μm^2) and 0.34 μA was supplied by the AH (area 408 μm^2).

The K_{DR} current density needed for membrane repolarization was ~730 pA/μm^2 at a voltage pulse from −70 to +20 mV in both the AH and IS. For simplicity, K_A channels were excluded from the model of the cat motoneuron.

The antidromic action potentials were simulated by the application of depolarizing 0.5-ms current pulses to the distal end of the IS. The strength of the pulses, except where mentioned, was just sufficient to reach the firing threshold in the modeled motoneuron.

RESULTS

Modeled currents

The Na^+ and K^+ currents simulated using the parameters given in the Materials and Methods section are shown in Fig. 1. The Na^+ currents had kinetics similar to those reported for rat neocortical pyramidal neurons (Huguenard et al., 1988), spinal motoneurons (Safronov and Vogel, 1995), and dorsal horn neurons (fast component; Safronov et al., 1997).

The steady-state inactivation parameters for Na^+ channels in dorsal horn neurons necessary for the model were determined in experiments with 11 isolated *somata* (not shown). These measurements were carried out on isolated *somata*, to minimize the voltage errors due to insufficient space clamp. E_{H50} and k values determined using 160-ms voltage prepulses were −78.3 ± 2.5 and 9.0 ± 0.7 mV, respectively. For spinal motoneurons the E_{H50} and k values were reported to be ~ −82 mV and ~10 mV, respectively (Safronov and Vogel, 1995). In the h_∞ equation of our model (see Materials and Methods), the E_{H50} parameters were set to −75 mV and k was set to 9 mV for both types of spinal neurons.

To illustrate the steady-state activation and inactivation ranges of modeled Na^+ and K^+ currents, we measured their amplitudes at different potentials, converted them into normalized conductances, and fitted these points using the Boltzmann equation (Fig. 1).

For simulated Na^+ currents, the activation curve for all neurons was best fitted with $E_{50} = -29.3$ mV and $k = 8.9$ mV. The fitting parameters for the steady-state inactivation curves were $E_{H50} = -64.4$ mV and $k = 5.9$ mV for pyramidal neuron and $E_{H50} = -74.3$ mV and $k = 9.4$ mV for both spinal neurons. Thus, at the resting potential of −70 mV used in our simulations (except those in Figs. 2 and 6–8), the portion of noninactivated Na^+ channels was 70% in pyramidal and 37% in spinal neurons.

For modeled K_A currents, the activation characteristic was best fitted with $E_{50} = -31.0$ mV and $k = 12.3$ mV. The steady-state inactivation was fitted with $E_{H50} = -85.0$ mV and $k = 10.2$ mV.

The steady-state activation of simulated K_{DR} currents was fitted with $E_{50} = -8.6$ mV and $k = 11.7$ mV.

Recording and simulation of the soma responses

The adequacy of the computer simulation method in describing the responses of the neuronal soma was tested in experiments with spinal dorsal horn neurons, in which the active and passive responses of an ESI-isolated soma (*soma*) and a simulated soma were compared (Fig. 2). After isolation, the *soma* has lost the majority of Na^+ channels and its ability to generate action potentials (Fig. 2, *left* and *middle*). Comparison of active (*solid line*) and passive (*dashed line*) responses of the isolated *soma* to depolarizing current pulses under current-clamp conditions indicated the presence of only a small local depolarization. In a modeled soma we have first adjusted the densities of passive (leakage) and voltage-dependent (Na^+, K_A, and K_{DR}) conductances to match R_{IN} and the amplitudes of currents originally recorded in a given isolated *soma* under voltage-clamp conditions. After switching the modeled soma to a current-clamp mode, we have controlled the time constant of pas-

sive membrane responses to hyperpolarizing current pulses. For an adequate fit of the passive current-clamp responses of the isolated *soma* shown in Fig. 2, the C_M of the simulated soma had to be increased from 1 to 2 $\mu F/cm^2$ (the influence of the C_M value on the results of our further simulations was tested in another section). The current-clamp response of the simulated soma to a depolarizing pulse is shown in Fig. 2 (*right*). It is seen that a computer simulation with appropriately adjusted parameters gave responses very similar to those originally recorded from the isolated *soma* in both voltage-clamp and current-clamp experiments.

Densities of Na^+ and K^+ channels in the soma of a motoneuron

Data on the densities of voltage-gated Na^+ and K^+ currents in the soma of rat motoneurons have not been available so far. Therefore, we performed experiments in which they were determined. Because the Na^+ channel density is the major factor determining membrane excitability, special precautions had to be taken for its correct estimation. Our previous study of dorsal horn neurons in spinal cord slices has shown that the estimations of somatic Na^+ channel densities performed in ESI experiments and in single-channel experiments using inside-out and cell-attached (but not outside-out) membrane patches are very close to each other (Safronov et al., 1997, and unpublished observations). Therefore, we determined the density of Na^+ and K^+ channels in the soma of a motoneuron by recording their activity in cell-attached patches. At the end of each experiment the patch membrane was ruptured and the resting potential was measured. The resting potentials of motoneurons (between -80 and -60 mV) were added to the command potential.

Na^+ channels were studied using pipettes filled with external TEA solution. The channels were activated by 50-ms voltage steps to different depolarizing test potentials after a 50-ms negative prepulse to -120 mV. Ten to forty consecutive traces were averaged at each test potential (Fig. 3 *A*), and the maximum averaged current (usually at -20 to 0 mV) was determined. The peak value of the averaged Na^+ current in 10 cell-attached patches was 6.1 $\pm$ 0.9 pA (no patch was empty, currents ranged from 1.9 to 11.2 pA). The mean pipette resistance was 2.7 $\pm$ 0.15 MΩ, giving a mean patch area of 4.9 μm^2 (Sakmann and Neher, 1995) and a Na^+ current density of 1.24 pA/μm^2.

As reported previously (Safronov and Vogel, 1995), transient K_A channels in the soma of rat motoneurons lost their fast inactivation kinetics ($\tau \approx 15$–60 ms) when studied in cell-attached or inside-out patches. Furthermore, the steady-state inactivation of K_A channels in cell-attached patches became incomplete, so that it was not possible to separate K_A and delayed-rectifier K_{DR} currents in cell-attached patches by a standard procedure with different prepulses. Therefore, the identification of K^+ channels was performed

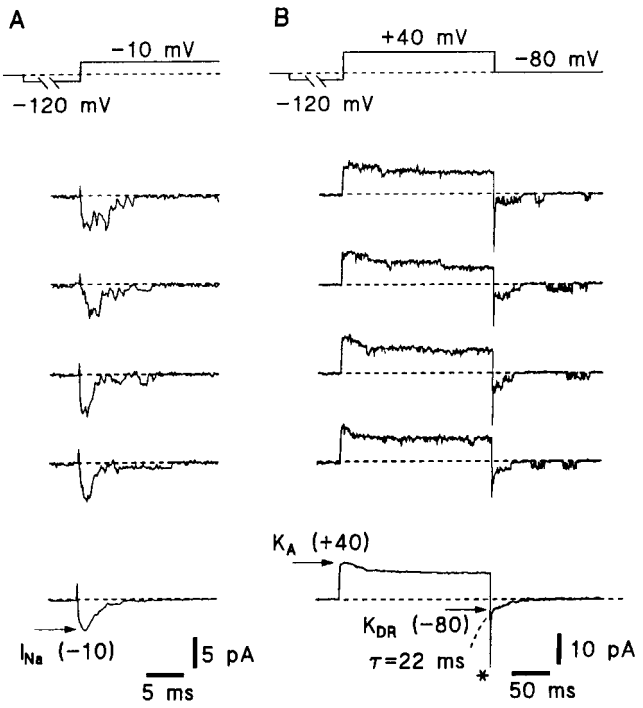

FIGURE 3 Densities of voltage-gated Na^+ and K^+ currents in the soma of rat motoneurons. (*A*) Na^+ channels were activated in cell-attached patches by a voltage pulse to ~ -10 mV after a hyperpolarizing 50-ms prepulse to ~ -120 mV. The lowermost trace represents the average of 20 recordings. The pipette solution was Ringer-TEA. (*B*) K^+ channels were activated in cell-attached patches by a voltage step to $\sim +40$ mV after a 150-ms prepulse to ~ -120 mV. The lowermost trace is an average of 20 recordings. The peak current at +40 mV was considered as K_A current. K_{DR} current was measured at a resting potential of ~ -80 mV as the amplitude of the slow component ($\tau = 22$ ms) of the tail current (*asterisk* indicates the fast component). The pipettes were filled with high-K_o solution. Temperature: 21–24°C.

in external high-K_o solution, and the current densities were then recalculated for physiological saline. The channels were activated by a 200-ms depolarizing voltage pulse to +40 mV after a 150-ms hyperpolarizing prepulse to -120 mV (Fig. 3 *B*). K_A current was measured as the peak outward K^+ current at +40 to +50 mV under the assumption that the contribution of slowly activating K_{DR} current is negligible. K_{DR} current was determined from the tail currents after the potential return to the resting potential of -80 to -70 mV (Fig. 3 *B*). The tail currents consisted of a fast ($\tau = 1$–3 ms, peak indicated by an *asterisk*) and a slow ($\tau \approx 20$ ms) component, corresponding to fast closure of K_A and slow closure of K_{DR} channels (Safronov and Vogel, 1995). The amplitude of the slow component of the tail current was considered to be K_{DR} current. In 12 cell-attached patches, the mean K_A current at +40 to +50 mV ($\sim +45$ mV) was 13.0 $\pm$ 2.9 pA, and K_{DR} current measured at -70 to -80 mV (~ -75 mV) was 4.1 $\pm$ 1.9 pA. The mean pipette resistance of 2.63 $\pm$ 0.18 MΩ (patch area of 5.0 μm^2) gave

current densities of 2.6 pA/μm^2 for K_A channels at +45 mV and 0.82 pA/μm^2 for K_{DR} at −75 mV. Using K_{DR} channel conductances of 31.1 pS for inward currents in symmetrical high-K^+ solutions (E_K = 0 mV) and 10.2 pS for outward currents in external physiological saline ($[K^+]_o$ = 5.6 mM, E_K = −84 mV), from Safronov and Vogel (1995), the density of K_{DR} currents in physiological saline at +45 mV was estimated to be 0.46 pA/μm^2. A similar reevaluation made for K_A channels, assuming their conductance of 39.6 pS for outward currents in symmetrical high-K^+ solution and 19.2 pS in physiological saline (Safronov and Vogel, 1995), gave a K_A current density in physiological saline of 3.6 pA/μm^2 at +45 mV. These data are in a good agreement with the results of our ESI experiments, showing that the somata of spinal neurons possess more K_A than K_{DR} currents, whereas K_{DR} channels are more strongly expressed in dendrites (Wolff et al., 1998).

Thus, according to our recordings from cell-attached patches the Na^+ current density in a model soma of spinal motoneuron was set to 1.24 pA/μm^2 at a voltage step from −120 to −10 mV. The K_A current density in a motoneuron was set to 3.6 pA/μm^2 at a voltage step from −120 to +45 mV. The density of K_{DR} current activated by a voltage step to +45 mV was 0.46 pA/μm^2.

Simulated somatic responses of central neurons

Responses of the somata of a dorsal horn neuron, a motoneuron, and a pyramidal neuron, simulated using the parameters given in Materials and Methods and Results, are shown in Fig. 4. The active membrane responses (*solid lines*) are compared with the passive responses (*dashed lines*). The latter were obtained by setting the voltage-gated Na^+ and K^+ conductances to zero. The responses of the soma of a dorsal horn neuron consisted of a large passive component with a small local depolarization, even at strong membrane depolarizations to ~0 mV. A similar type of membrane response to current injection was simulated for the soma of a motoneuron. In contrast to those of both spinal neurons, the soma of the pyramidal neuron was able to generate an action potential with an overshoot of +9 mV.

To test whether our conclusions about the inability of the somata of spinal neurons to generate spike potentials can be influenced by the major parameters determining the passive membrane properties, some simulations were performed in which C_M, R_i, and R_m (R_{IN}) values were varied in a broad range. Increasing the C_M from 1 to the value of 2.4 μF/cm^2 reported for the spinal neurons studied by the patch-clamp technique in slice preparation (Thurbon et al., 1998) resulted in a further decrease in the amplitude of the local depolarization in the soma of both spinal neurons. Varying R_i in the range between 50 and 200 Ω cm produced no remarkable changes in the shape of the response of the somata. This insensitivity of modeled responses to R_i could be simply explained by a small electrotonic length of the somata (<0.02λ). A 10-fold increase in the R_m value to 222,220 Ω cm^2 for a dorsal horn neuron and to 121,210 Ω cm^2 for a motoneuron, corresponding to an increase in R_{IN} to 70 and 6 GΩ, respectively, did not make the modeled somata of either spinal neuron able to generate spike potentials. Therefore, it could be assumed that the low density of Na^+ channels is the major reason for the nonexcitability of the somata in both spinal neurons.

What does the soma of a spinal neuron need to become excitable?

In the following simulations we studied an increase in the density of Na^+ channels necessary to make the somata of both spinal neurons able to generate action potentials. The densities of somatic Na^+ channels were increased by factors of 2, 4, and 8 (Fig. 5). A twofold increase in channel density amplified the local responses in both somata. A fourfold increase resulted in the appearance of overshoots (+17 mV

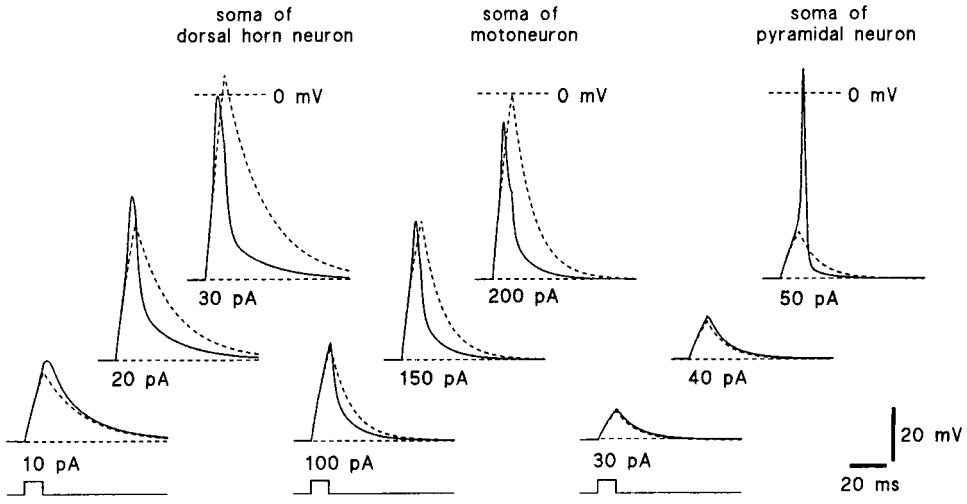

FIGURE 4 Simulated responses of somata. Simulated responses of somata of a dorsal horn neuron, a motoneuron, and a pyramidal neuron to 10-ms current pulses of increasing strength. The resting potential was −70 mV. Passive membrane responses obtained by setting all active conductances to zero are shown by dashed lines.

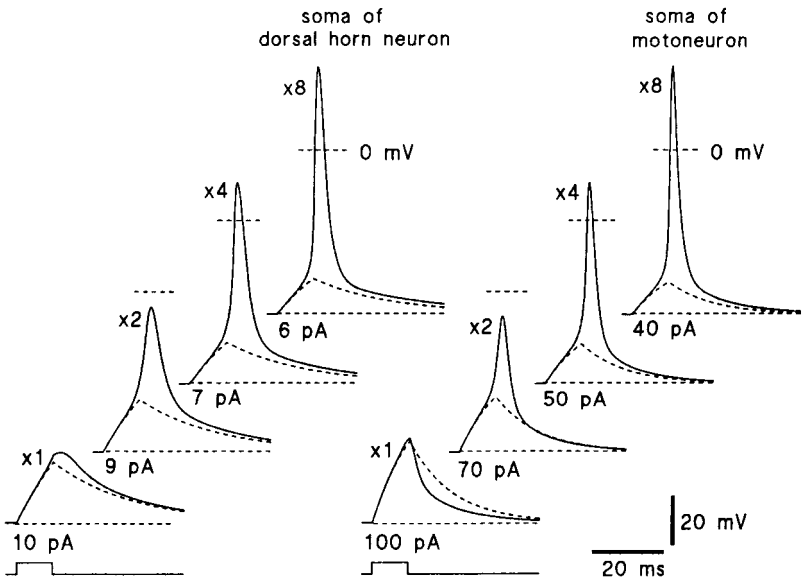

FIGURE 5 An increase in Na^+ channel density makes the soma of spinal neurons excitable. Shown are responses of the somata of a dorsal horn neuron and a motoneuron to 10-ms current pulses of different strengths (indicated near the corresponding traces). The resting potential was −70 mV. The lowermost traces show responses of the somata, with Na^+ channel densities determined experimentally. The following traces show simulated responses of somata with Na^+ channel densities increased by factors of 2, 4, and 8. Passive membrane responses are shown by dashed lines. The levels of 0 mV are indicated by horizontal dashed lines.

in the dorsal horn neuron and +16 mV in the motoneuron), but the velocity of depolarization remained low. Finally, an increase in Na^+ channel density by a factor of 8 lowered the firing threshold, increased the velocity of depolarization, and increased the overshoots to ~ +40 mV. Thus a four- to eightfold increase in the density of Na^+ channels was necessary to make the somata of the dorsal horn neuron and motoneuron excitable. If the densities of Na^+, K_A, and K_{DR} channels were increased simultaneously, then an 8–16-fold increase in the channel densities was needed for the appearance of somatic excitability (not shown).

Simulation of action potentials in an adult cat motoneuron

In the classical experiments with adult cat motoneurons, Coombs et al. (1957a) observed that the antidromic spikes recorded intrasomatically with a sharp electrode consisted of two major components. The fast component with an amplitude of 30–40 mV was postulated to be passively produced in the somatic membrane by a 80–100-mV spike invading the axon initial segment, whereas the slower component was an all-or-nothing spike generated by the soma itself. These conclusions were further supported in experiments by Araki and Terzuolo (1962), as well as by pioneering computer simulations of action potentials in a cat motoneuron performed by Dodge and Cooley (1973). The idea of axonal and somatic origin of the two components of the action potential was based on several important observations: 1) By inserting the recording electrode into different positions within the soma and axon initial segment of one motoneuron, it was possible to record spike potentials with varying proportions of the fast and slow components (Coombs et al., 1957a). 2) The threshold of the fast component was 10–20 mV lower than that of the slower one (Coombs et al., 1957b). 3) An injection of a hyperpolarizing current into the soma of some motoneurons could induce a blockage of the slow component of an antidromically evoked action potential, whereas the small fast component still invaded the soma (Coombs et al., 1955). 4) Voltage clamp of the soma membrane at its resting potential prevented the antidromic invasion of the action potential into the soma; under these conditions an inward Na^+ current of 0.12 μA causing the spike in the unclamped membrane of the axon initial segment could be seen in the soma (Araki and Terzuolo, 1962).

This interpretation of spike potential in a motoneuron is in contradiction to the results of the present paper showing inexcitability of the soma in spinal neurons. Therefore, we performed the following simulations, to test whether the antidromically evoked two-component action potential could originate from a complex geometry of the axon hillock (AH) and initial segment (IS) and whether the experimental observations mentioned above could be simulated using a model of a motoneuron with an inexcitable soma.

The model of an adult cat motoneuron based on the parameters given in Materials and Methods is shown in Fig. 6 *A*. It consisted of the soma, AH, axon IS, and an equivalent dendrite. Voltage-gated Na^+ and K_{DR} conductances were inserted into the membrane of AH and IS only (indicated by *black*). For simplicity, the soma and an equivalent dendrite were equipped with passive conductances only. The antidromic invasion of an action potential into the soma was simulated by injecting 0.5-ms depolarizing currents into the distal part of the IS, as indicated by a filled arrowhead. The action potentials calculated for different points along the IS, AH, and soma are shown in Fig. 6 *B*. It is seen that the spike potentials consist of two components, a fast

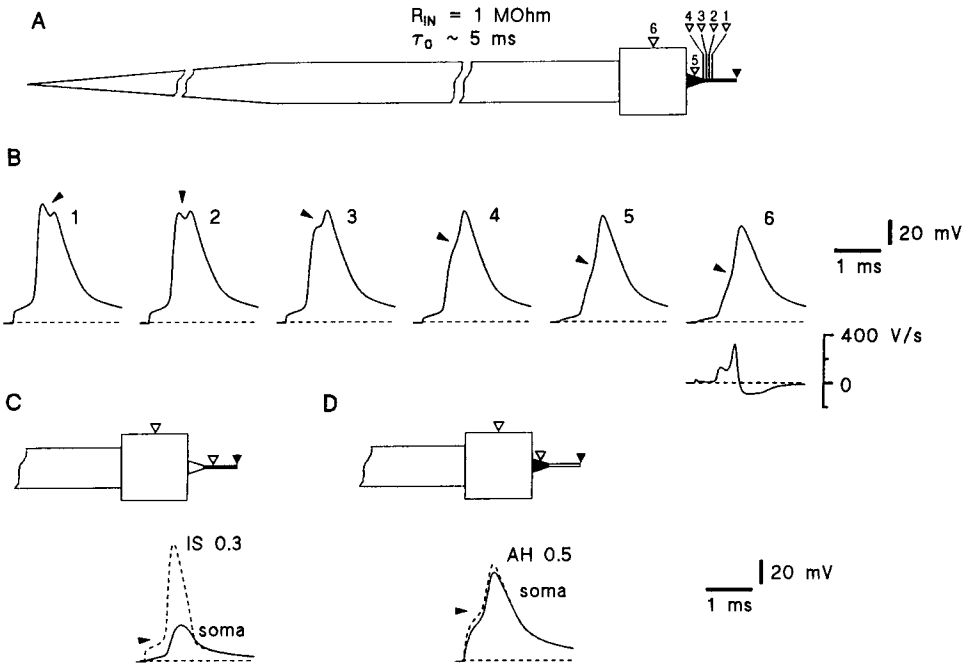

FIGURE 6 Simulation of spikes in a cat motoneuron. (*A*) Model of a motoneuron constructed using parameters given in Materials and Methods. The motoneuron consisted of a soma, an axon hillock (AH), an axon initial segment (IS), and an equivalent dendrite. Soma and dendrite possessed only passive conductances. The AH and IS also contained active (Na^+ and K_{DR}) conductances (indicated by *filled segments*). The points of stimulations (the distal end of the IS) and recordings are indicated by filled and open arrowheads, respectively. (*B*) Simulations of the spike potentials along the IS, AH, and soma. Simulation points were 1 at IS (0.3, assuming 0 as the left end and 1 as the right end), 2 at IS (0.2), 3 at IS (0.1), 4 at AH (1), 5 at AH (0.5), and 6 at the soma (0.5). The arrowheads indicate a transition between fast and slow components of the spike. A differentiated trace of the response calculated for the soma is shown below. (*C*) Spike potentials calculated for the soma (0.5, *solid line*) and IS (0.3, *dashed line*) after removal of Na^+ channels from the AH. (*D*) Spikes in the soma (0.5, *solid line*) and AH (0.5, *dashed line*) simulated after removal of Na^+ channels from the IS. In *C* and *D* the arrowheads show the spike thresholds.

and a slow (the *arrows* indicate the transitions), and that the proportion of the fast component decreases as the spike potential approaches the soma. The contribution of both components became equal in the proximal part of the IS (*point 2*), giving a spike shape similar to that of figure 4 *A* of Coombs et al. (1957a). The slow spike component already dominated over the fast one at the border between IS and AH (*points 3 and 4*), the spike at point 3 being very similar to that shown in figure 5 *A* of Coombs et al. (1957a) for the electrode position relatively close to the soma. The spikes calculated for the middle of the AH (*point 5*) and the soma (*point 6*) were almost indistinguishable from each other; both showed the dominance of the slower component. A differentiated trace of the action potential calculated for the soma (Fig. 6 *B, point 6, bottom*) showed a maximum velocity of depolarization (320 V/s) and the interval between invasions of the two components (0.3 ms), which are in good agreement with experimental data reported for cat motoneurons (Coombs et al., 1957a).

To determine the origin of both components of somatic spike simulated with our model, the densities of Na^+ channels either in the AH or in the IS were set to zero, while all other parameters remained unchanged. Removal of Na^+ channels from the AH resulted in a disappearance of the slow spike component (Fig. 6 *C*). The remaining fast component displayed a low amplitude and a low threshold of activation (*filled arrowhead*), being passively produced in the soma by the action potential generated in the IS (*dotted line*). Removal of Na^+ channels from the IS led to a disappearance of the fast component (Fig. 6 *D*) and to a considerable increase in the threshold of spike potential. Thus the two components of the spike potential seen in the soma of our model represented the spikes generated in the IS and AH.

Gradual hyperpolarization of the modeled motoneuron by setting the equilibrium potential of the passive conductance to −90, −95, and −100 mV resulted in a more pronounced inflection on the rising phase of the spike and, finally, in complete blockage of the slow component (Fig. 7, left). This blockage was very similar to that experimentally observed by Coombs et al. (1955, Fig. 7) and simulated by Dodge and Cooley (1973, Fig. 7), using the motoneuron model with an excitable soma. It was also reported that in many motoneurons it was not possible to produce a blockage of the slow component, whatever hyperpolarizing currents were used (Coombs et al., 1955; K. E. Jones, personal communication). Our model gives several possibilities for reproducing

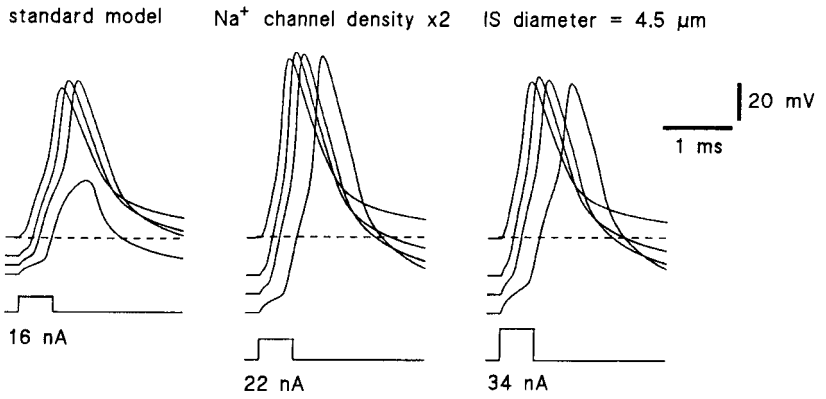

FIGURE 7 Blockage of the slower component of the spike by hyperpolarization. (*Left*) Antidromic spikes simulated in the soma under standard conditions and after hyperpolarization by 10, 15, and 20 mV. (*Middle*) Spikes seen during the membrane hyperpolarization by 20, 30, and 40 mV in the model where the Na^+ channel density in both IS and AH was twice increased. (*Right*) Spike potentials after the membrane hyperpolarization by 20, 30, and 40 mV in the model with a normal density of Na^+ channels but an increased IS diameter from 3.5 to 4.5 μm.

these observations. By twice increasing the density of the Na^+ channels in the membrane of AH and IS, action potentials were simulated that could not be suppressed by membrane hyperpolarization to up to −120 mV (Fig. 7, *middle*). Another possibility was to increase the diameter of the axon IS (the diameter of the distal part of the AH was correspondingly increased). Anatomical measurements give IS diameters ranging from 2.3 to 4.9 μm (mean 3.5 μm; Cullheim and Kellerth, 1978). An increase in the IS diameter from 3.5 to 4.5 μm in a modeled motoneuron resulted in a spike potential that was not blocked by hyperpolarization (Fig. 7, *right*). In many motoneurons, Coombs et al. (1955) also observed that complete antidromic spikes already failed to invade the soma at the resting potential. In these cases, the spike potential in the soma consisted of the small fast component only. We could reproduce these observations, for example, by setting the IS diameter in the model to 2.9 μm (not shown). In general, lowering the R_m value for the soma membrane (corresponding to an increase in the somatic shunt introduced by the recording electrode) or decreasing the density of Na^+ channels as well as the IS diameter introduced a stronger inflection on the rising phase of the spike and made blockage of the slow component easier.

The simulations reproducing the major observations of Araki and Terzuolo (1962) are shown in Fig. 8. Under current-clamp conditions, no current was recorded in the soma (Fig. 8 *A*), as a two-component antidromic spike invaded both the IS (Fig. 8 *B, thin line*) and the soma (Fig. 8 *B, thick line*). Switching the soma electrode to the voltage-clamp mode and holding the somatic membrane at a potential of −80 mV resulted in a disappearance of the slow component of antidromic spike generated in the IS (Fig. 8 *D, thin line*) and in a complete disappearance of the spike potential in the soma (Fig. 8 *D, thick line*). Under these conditions, a ~0.1-μA inward Na^+ current could be seen in the soma (Fig. 8 *C*). To determine the origin of this current, we have set the Na^+ channel density in the IS to zero, while the channel density in the AH remained unchanged. This resulted in a disappearance of both the inward current in the soma and the fast spike potential in the IS (Fig. 8, *C* and *D*, *dashed lines*).

Thus the model of a motoneuron with a passive soma is also able to reproduce major experimental observations, which had led Coombs et al. (1957a) to their conclusion about the excitability of the somatic membrane. The low density of Na^+ channels found in the soma membrane of an intact motoneuron can only slightly increase the amplitude of the slow spike component generated by the AH.

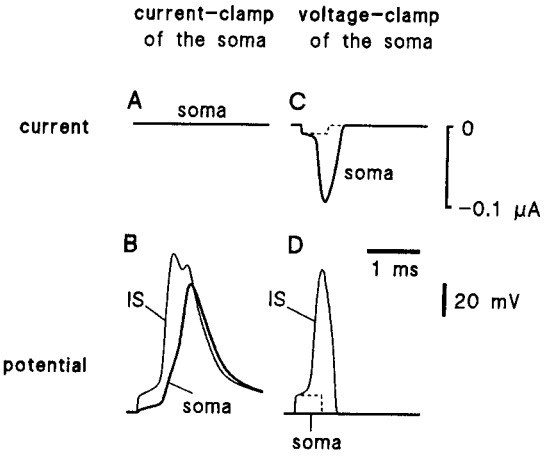

FIGURE 8 Simulation of observations from Araki and Terzuolo (1962). (*A* and *B*) Current clamp of the soma during antidromic spike invasion. (*A*) Currents flowing into the soma during the invasion. (*B*) Simulated voltage recordings from the soma (*thick line*) and IS (0.3, *thin line*). (*C* and *D*) Voltage clamp of the soma membrane at its resting potential during antidromic invasion of the spike. (*C*) Inward Na^+ currents in a voltage-clamped soma appearing when the spike invades the IS. The thin dashed line shows membrane currents after the Na^+ channel density in the IS (but not in AH) is set to zero. (*D*) Voltage changes in the soma (*thick line*) and in the IS (0.3, *thin line*) during spike invasion. The thin dashed line shows voltage changes in the IS (0.3) after the Na^+ channel density in the IS is set to zero.

DISCUSSION

We studied the ability of the somata of three different CNS neurons to generate action potentials. The small soma of the spinal dorsal horn neuron, with a diameter of ~10 μm, separated from its axon and dendrites by means of the ESI method (Safronov et al., 1997), has proved to be a convenient model for the study of somatic excitability. A computer simulation method tested with the isolated *soma* of a dorsal horn neuron was employed to describe the excitability of larger somata of a motoneuron and hippocampal pyramidal neuron, which, because of their tight connections to the surrounding tissue, could not be directly isolated by the ESI method.

Excitability of the soma

Our simulations have shown that the soma of the hippocampal pyramidal neuron but not of spinal neurons is able to generate spikes. Inexcitability of the somata of both spinal neurons resulted from a relatively low density of voltage-gated Na^+ currents: 0.87 pA/μm^2 in the dorsal horn neuron and 1.24 pA/μm^2 in the motoneuron versus 3 pA/μm^2 in the pyramidal neuron. This lower channel density in spinal neurons is unlikely to result from using younger animals in our experiments, 2–15 days for spinal neurons (Safronov et al., 1997; Materials and Methods) versus 2–8 weeks for pyramidal neurons from Colbert and Johnston (1996), because the density of somatic Na^+ channels in spinal neurons does not increase during the first 39 days of postnatal development (Safronov et al., 1999). Another reason for a lower excitability of the soma in spinal neurons was a stronger inactivation of Na^+ channels at the resting potential (Safronov and Vogel, 1995; Results), in comparison with the pyramidal neuron (Huguenard et al., 1988). The higher density of K_A and K_{DR} channels in the soma of the pyramidal neuron influenced the shape of the spike but had no effect on the ability of the soma to generate action potentials.

It is interesting to note that the somatic Na^+ conductance in the spinal and pyramidal neurons seems to follow different courses of postnatal development. A significant increase in Na^+ channel density was observed in the soma of pyramidal neurons during the first weeks of maturation (Huguenard et al., 1988; Alzheimer et al., 1993). In contrast, the soma of the spinal neuron did not experience a remarkable increase in the Na^+ channel density during the first postnatal month (Safronov et al., 1999), a period of development when most changes in Na^+ channel expression occur (Beckh et al., 1989).

Why can't the soma initiate a spike?

According to a classical point of view, action potentials are initiated in the axon and then propagate to the soma and dendrites (Coombs et al., 1957a,b; Eccles, 1964; Stuart and Sakmann, 1994; Safronov, 1999). The present results allow us to discuss why the somata of CNS neurons cannot initiate spikes.

In spinal neurons the soma itself (without the axon initial segment) was not able to generate a spike. The density of Na^+ channels was four to eight times lower than the value necessary for the appearance of excitability. The soma of spinal neurons did not become excitable during postnatal development, which was accompanied by additional expression of Na^+ channels in the axonal but not in the somatic membrane (Safronov et al., 1999). Thus the axon seems to be the only structure in the spinal neuron where spike potentials can be generated.

In contrast to spinal neurons, the soma of a hippocampal pyramidal neuron can generate spikes. It does not initiate a spike in an intact neuron where the majority of Na^+ channels are located in a narrow membrane region of the axon initial segment (Catterall, 1981; Boudier et al., 1985; Wollner and Catterall, 1986; Angelides et al., 1988; Safronov et al., 1997) with a large ratio of Na^+ conductance to the passive capacitive load. Such a localization of Na^+ channels in the axon initial segment results in a lowering of the firing threshold, which makes the axon initial segment a favorable site for spike initiation in the pyramidal neuron.

Spike potentials in adult cat motoneurons

Our conclusion about the inexcitability of the soma of spinal neurons in young rats disagrees with the interpretation of the spike potential made by Coombs et al. (1957a), who postulated that a larger (slow) component of the spike in the motoneuron of the adult cat is produced by the somatodendritic membrane. Using this interpretation of the spike, Dodge and Cooley (1973) created the first computer simulation of the action potential in the motoneuron and found that the experimental observations could be better reproduced if a model with inexcitable dendrites was used, suggesting that the slow spike component was generated by the soma alone. In this case, the soma would have to "drive" a large passive load of the dendritic tree and, therefore, would have to be equipped with Na^+ channels at densities much higher than those predicted from our model of the soma "separated" from dendrites (see Fig. 5, control density $\times 8$). To reproduce the experimental observations, Dodge and Cooley had to use a very high density of somatic Na^+ channels, which was just only 8.6 times lower than that in the axon initial segment. On the one hand, such a density of Na^+ channels would be much higher than the values of 1–4 μm^{-2} measured in the somata of different CNS neurons so far (MacDermott and Westenbrook, 1986; Colbert and Johnston, 1996; Safronov et al., 1997), on the other hand, the experimentally determined ratio of axonal to somatic density of Na^+ channels was at least 160 for spinal neurons (1 μm^{-2} in the soma versus 160 μm^{-2} in the axon initial

segment; Safronov et al., 1999), and, therefore, the value of 8.6 used by Dodge and Cooley represents an overestimation of somatic channel density. Furthermore, somatic Na^+ conductance in Dodge and Cooley's model, calculated as (membrane area) $\times$ (conductance density, g_{NA}), was 2.1 times larger than that of the axon initial segment, whereas our recent ESI experiments have shown that the proportion of the somatic component in total Na^+ current recorded in an intact spinal neuron decreases with age, being only 4.2% for 39-day-old animals (Safronov et al., 1999).

Although the possibility still cannot be excluded that the differences in animal species and age are the major reasons for the discrepancies mentioned above, we have attempted to determine whether the slow component of the action potential could be produced by the AH rather than by the soma. Our model with a passive soma and excitable AH and IS could reproduce the major experimental observations that had led Coombs et al. (1957a) to their conclusions about the excitability of the soma. A tapering AH and cylindrical IS, reconstructed in accordance with anatomical measurements of cat motoneurons, were critical for the appearance of two-component spikes. The AH was tightly coupled electrotonically to the soma, so that the spike potentials in the soma and AH were almost indistinguishable from each other. In this case, recording with an intrasomatic electrode would not provide a way of distinguishing between a somatic or AH origin of the slow spike component.

The idea of the Na^+ channel localization in the axonal segment adjacent to the soma is supported by several reports (Catterall, 1981; Wollner and Catterall, 1986; Safronov et al., 1997, 1999). The present study has further shown that the geometry of the axon has a stronger influence on the spike shape than has been supposed so far. A relatively large base diameter of the AH provided its better electrotonical coupling to the soma than to the IS. Similar results would also be obtained if Na^+ channels were localized in a narrow region of the soma just surrounding the AH. Although the data available at the moment give no way of exactly determining the Na^+ channel distribution in the motoneuron of adult cats as well as distinguishing between our model and the Dodge-Cooley model of spike generation, we have shown that two-component spikes can be generated by the initial part of the axon, and that the observation of Coombs et al. (1957a) could be reproduced using a model with an inexcitable soma.

Relevance of the soma behavior for neuronal firing

The properties of somata can have a strong influence on the spike propagation in CNS neurons. The soma of the hippocampal pyramidal neuron, with a relatively high density of Na^+ channels and its capacity for spike generation, can actively support the back-propagation of action potentials from the axon initial segment to dendrites (Stuart and Sakmann, 1994), providing a feedback mechanism of excitability. In contrast, the somata of spinal neurons, with a lower density of Na^+ channels, seem to play a classic integrative role. By local depolarization, somata can amplify the excitatory postsynaptic potentials on their way to the axon initial segment but may reduce the spike back-propagation from the axon to dendrites (Wolff et al., 1998; Safronov, 1999).

We thank Dr. M. E. Bräu for critical discussions and comments on the manuscript, Dr. K. E. Jones for helpful discussions and advice concerning simulations, Mrs. B. Agari for excellent technical assistance, and Mr. J. Beltzer for help with computer simulation.

The work was supported by the Deutsche Forschungsgemeinschaft (DFG Vo188/16).

REFERENCES

Alzheimer, C., P. C. Schwindt, and W. E. Crill. 1993. Modal gating of Na^+ channels as a mechanism of persistent Na^+ current in pyramidal neurons from rat and cat sensorimotor cortex. *J. Neurosci.* 13:660–673.

Angelides, K. J., L. W. Elmer, D. Loftus, and E. Elson. 1988. Distribution and lateral mobility of voltage-dependent sodium channels in neurons. *J. Cell Biol.* 106:1911–1925 (erratum: 108:2001).

Araki, T., and C. A. Terzuolo. 1962. Membrane currents in spinal motoneurons associated with the action potential and synaptic activity. *J. Neurophysiol.* 25:772–789.

Barrett, J. N., and W. E. Crill. 1974. Specific membrane properties of cat motoneurones. *J. Physiol. (Lond.).* 239:301–324.

Beckh, S., M. Noda, H. Lubbert, and S. Numa. 1989. Differential regulation of three sodium channel messenger RNAs in the rat central nervous system during development. *EMBO J.* 8:3611–3616.

Boudier, J. A., Y. Berwald-Netter, H. D. Dellmann, J. L. Boudier, F. Couraud, A. Koulakoff, and P. Cau. 1985. Ultrastructural visualization of Na^+-channel associated [^{125}I]alpha-scorpion toxin binding sites on fetal mouse nerve cells in culture. *Brain Res.* 352:137–142.

Burke, R. E., and G. ten Bruggencate. 1971. Electrotonic characteristics of alpha motoneurones of varying size. *J. Physiol. (Lond.).* 212:1–20.

Catterall, W. A. 1981. Localization of sodium channels in cultured neural cells. *J. Neurosci.* 1:777–783.

Clements, J. D., and S. J. Redman. 1989. Cable properties of cat spinal motoneurones measured by combining voltage clamp, current clamp and intracellular staining. *J. Physiol. (Lond.).* 409:63–87.

Colbert, C. M., and D. Johnston. 1996. Axonal action-potential initiation and Na^+ channel densities in the soma and axon initial segment of subicular pyramidal neurons. *J. Neurosci.* 16:6676–6686.

Coombs, J. S., D. R. Curtis, and J. C. Eccles. 1957a. The interpretation of spike potentials of motoneurones. *J. Physiol. (Lond.).* 139:198–231.

Coombs, J. S., D. R. Curtis, and J. C. Eccles. 1957b. The generation of impulses in motoneurones. *J. Physiol. (Lond.).* 139:232–249.

Coombs, J. S., J. C. Eccles, and P. Fatt. 1955. The electrical properties of the motoneurone membrane. *J. Physiol. (Lond).* 130:291–325.

Cullheim, S., and J. O. Kellerth. 1978. A morphological study of the axons and recurrent axon collaterals of cat sciatic alpha-motoneurons after intracellular staining with horseradish peroxidase. *J. Comp. Neurol.* 178:537–557.

Dodge, F. A., and J. W. Cooley. 1973. Action potential of motoneuron. *IBM J. Res. Dev.* 17:219–229.

Eccles, J. C. 1964. The Physiology of Synapses. Springer-Verlag, Berlin, Göttingen, and Heidelberg.

Edwards, F. A., A. Konnerth, B. Sakmann, and T. Takahashi. 1989. A thin slice preparation for patch clamp recordings from neurones of the mammalian central nervous system. *Pflügers Arch.* 414:600–612.

Fleshman, J. W., I. Segev, and R. B. Burke. 1988. Electrotonic architecture of type-identified alpha-motoneurons in the cat spinal cord. *J. Neurophysiol.* 60:60–85.

Frankenhaeuser, B., and L. E. Moore. 1963. The effect of temperature on the sodium and potassium permeability changes in myelinated nerve fibres of *Xenopus laevis*. *J. Physiol. (Lond.).* 169:431–437.

Hamill, O. P., A. Marty, E. Neher, B. Sakmann, and F. J. Sigworth. 1981. Improved patch-clamp techniques for high-resolution current recording from cells and cell-free membrane patches. *Pflügers Arch.* 391:85–100.

Hille, B. 1992. Classical biophysics of the squid axon. *In* Ionic Channels of Excitable Membranes. B. Hille, editor. Sinauer Associates, Sunderland, MA. 23–58.

Hines, M. L. 1993. Neuron—a program for simulation of nerve equation. *In* Neural Systems: Analysis and Modeling. F. H. Eeckman, editor. Kluwer Academic Publishers, Boston.127–136.

Hines, M. L., and N. T. Carnevale. 1997. The NEURON simulation environment. *Neural Comput.* 9:1179–1209.

Hodgkin, A. L., and A. F. Huxley. 1952. A quantitative description of membrane current and its application to conduction and excitation in nerve. *J. Physiol. (Lond.).* 117:500–544.

Hoffman, D. A., J. C. Magee, C. M. Colbert, and D. Johnston. 1997. K^+ channel regulation of signal propagation in dendrites of hippocampal pyramidal neurons. *Nature.* 387:869–875.

Huguenard, J. R., O. P. Hamill, and D. A. Prince. 1988. Developmental changes in Na^+ conductances in rat neocortical neurons: appearance of a slowly inactivating component. *J. Neurophysiol.* 59:778–795.

Johnston, D., J. C. Magee, C. M. Colbert, and B. R. Christie. 1996. Active properties of neuronal dendrites. *Annu. Rev. Neurosci.* 19:165–186.

Jonas, P., G. Major, and B. Sakmann. 1993. Quantal components of unitary EPSCs at the mossy fibre synapse on CA3 pyramidal cells of rat hippocampus. *J. Physiol. (Lond.).* 472:615–663.

Jones, K. E., and P. Bawa. 1997. Computer simulation of the responses of human motoneurons to composite 1A EPSPS: effects of background firing rate. *J. Neurophysiol.* 77:405–420.

Kellerth, J. O., C. H. Berthold, and S. Conradi. 1979. Electron microscopic studies of serially sectioned cat spinal alpha-motoneurons. III. Motoneurons innervating fast-twitch (type FR) units of the gastrocnemius muscle. *J. Comp. Neurol.* 184:755–767.

Klee, R., E. Ficker, and U. Heinemann. 1995. Comparison of voltage-dependent potassium currents in rat pyramidal neurons acutely isolated from hippocampal regions CA1 and CA3. *J. Neurophysiol.* 74: 1982–1995.

MacDermott, A. B., and G. L. Westenbrook. 1986. Early development of voltage-dependent sodium currents in cultured mouse spinal cord neurons. *Dev. Biol.* 113:317–326.

Mainen, Z. F., J. Joerges, J. R. Huguenard, and T. J. Sejnowski. 1995. A model of spike initiation in neocortical pyramidal neurons. *Neuron.* 15:1427–1439.

Rall, W. 1959. Branching dendritic trees and motoneuron membrane resistivity. *Exp. Neurol.* 1:491–527.

Rall, W. 1969. Time constants and electrotonic length of membrane cylinders and neurons. *Biophys. J.* 9:1483–1508.

Safronov, B. V. 1999. Spatial distribution of Na^+ and K^+ channels in spinal dorsal horn neurones: role of the soma, axon and dendrites in spike generation. *Prog. Neurobiol.* 59:217–241.

Safronov, B. V., and W. Vogel. 1995. Single voltage-activated Na^+ and K^+ channels in the somata of rat motoneurones. *J. Physiol. (Lond.).* 487:91–106.

Safronov, B. V., M. Wolff, and W. Vogel. 1997. Functional distribution of three types of Na^+ channel on soma and processes of dorsal horn neurones of rat spinal cord. *J. Physiol. (Lond.).* 503:371–385.

Safronov, B. V., M. Wolff, and W. Vogel. 1999. Axonal expression of sodium channels in rat spinal neurones during postnatal development. *J. Physiol. (Lond.).* 514:729–734.

Sakmann, B., and E. Neher. 1995. Geometric parameters of pipettes and membrane patches. *In* Single-Channel Recording. B. Sakmann and E. Neher, editors. Plenum Press, New York. 637–650.

Stuart, G., and M. Hausser. 1994. Initiation and spread of sodium action potentials in cerebellar Purkinje cells. *Neuron.* 13:703–712.

Stuart, G. J., and B. Sakmann. 1994. Active propagation of somatic action potentials into neocortical pyramidal cell dendrites. *Nature.* 367:69–72.

Takahashi, T. 1990. Membrane currents in visually identified motoneurones of neonatal rat spinal cord. *J. Physiol. (Lond.).* 423:27–46.

Thurbon, D., H. R. Luscher, T. Hofstetter, and S. J. Redman. 1998. Passive electrical properties of ventral horn neurons in rat spinal cord slices. *J. Neurophysiol.* 80:2485–2502.

Ulfhake, B., and J. O. Kellerth. 1983. A quantitative morphological study of HRP-labelled cat alpha-motoneurones supplying different hindlimb muscles. *Brain Res.* 264:1–19.

Wolff, M., W. Vogel, and B. V. Safronov. 1998. Uneven distribution of K^+ channels in soma, axon and dendrites of rat spinal neurones: functional role of the soma in generation of action potentials. *J. Physiol. (Lond.).* 509:767–776.

Wollner, D. A., and W. A. Catterall. 1986. Localization of sodium channels in axon hillocks and initial segments of retinal ganglion cells. *Proc. Natl. Acad. Sci. USA.* 83:8424–8428.